Supplementary Materials for

Continuous monitoring of nighttime light changes based on daily NASA's Black Marble product suite

Tian Li[1,*], Zhe Zhu[1], Zhuosen Wang[2,3], Miguel O. Román[4], Virginia L. Kalb[2], Yongquan Zhao[1]

[1] Department of Natural Resources and the Environment, University of Connecticut, CT 06269, USA

[2] Terrestrial Information Systems Laboratory, NASA Goddard Space Flight Center, Greenbelt, MD 20771, USA

[3] Earth System Science Interdisciplinary Center, University of Maryland, College Park, MD 20740, USA

[4] Leidos Civil Group, Integrated Missions Operation, Reston, VA 20190, USA

* Corresponding author: Tian Li, tianli@uconn.edu

This file includes:

Figures S1 to S5, Tables S1 to S2, and detailed descriptions for cloud/snow buffer moving window size, stratification of VZA intervals, change detection parameter optimization, consistent dark pixel removal, and statistics of the validation samples.

1. Cloud/snow buffer moving window size

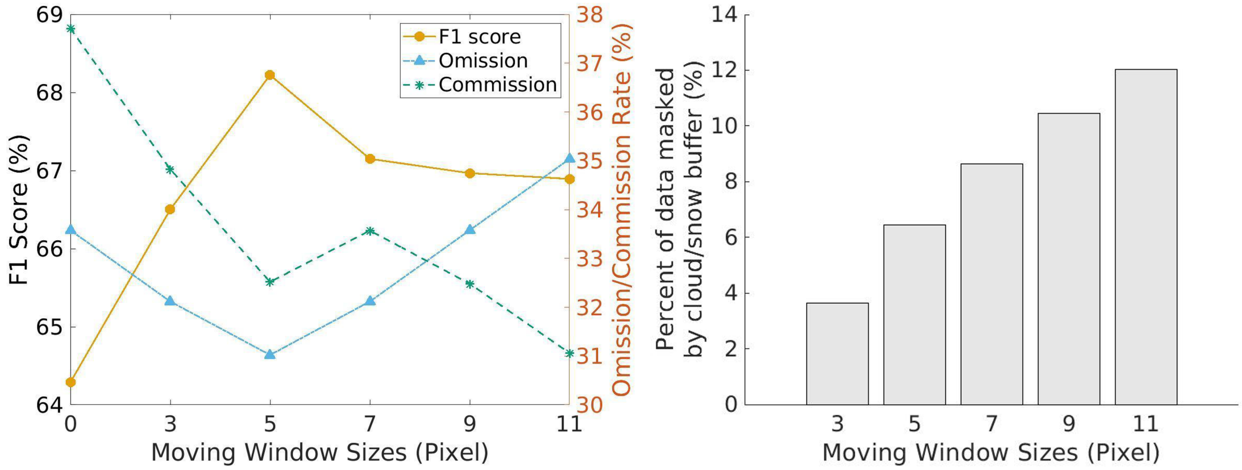

(a) (b)

Fig. S1. Analysis of the optimal cloud/snow buffer moving window size. (a) Accuracies for cloud/snow buffer at different moving window sizes. (b) The percent of data masked by the cloud/snow buffer for images collected at the eight titles at different moving window sizes.

2. Stratification of VZA intervals

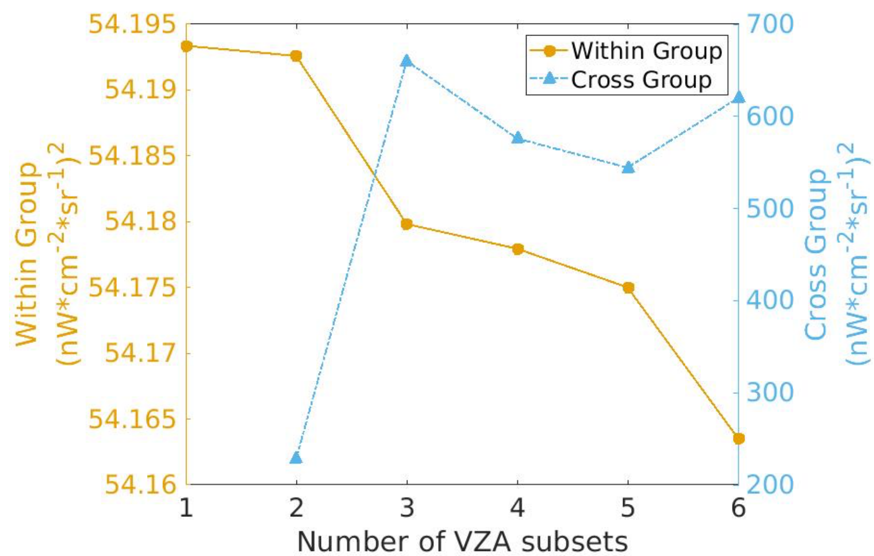

Fig. S2. The within-group standard deviation and cross-group standard deviation for the DNB observations equally divided (based on VZA) from two to six VZA subsets. DNB: Day/Night Band VZA: View Zenith Angle.

3. Change detection parameter optimization

We tested and compared the algorithm performance with different sets of parameters, one set for the all data interval (0-60°) and another set for the other three VZA subset intervals (0-20°, 20°-40°, 40°-60°), in which, the tested number of consecutive anomaly observations are 10, 12, 14, 16, 18, 20, and the tested change probabilities are 60%, 65%, 70%, 75%, 80%, 85%, 90%. Considering the data density of the all data interval (0-60°) is always higher than the other subsets and considering that the VZA stratification can reduce the temporal variation, here, we utilized rules that: (i) the number of consecutive anomaly observation for the all data interval should always be equal or larger than the ones applied to the VZA subset intervals; (ii) the change probability for the all data interval should always be equal or smaller than the ones applied to the VZA subset intervals. Based on the two rules, we run all different possible scenarios (a total of 588 scenarios) for the two parameters and the table below shows the top 9 scenarios (ranked by F1 score) evaluated based on the calibration data. Compared to the VZA-COLD with the same parameters among all VZA intervals (first row), the VZA-COLD with different sets of parameters for the all data interval and VZA subset intervals only improved the optimal F1 scores by less than 2%, but at the sacrifice of a higher omission error (omission error is usually considered more serious than commission error for change detection). Moreover, the smaller the number of consecutive observations to confirm a change, the faster a change can be confirmed. Thus, we decided to keep using the same number of consecutive anomaly observations of 14 and the change probability of 75% among all VZA intervals for the VZA-COLD.

Table S1. The top 9 ranked scenarios (based on the F1 score) of the VZA-COLD algorithm with different sets of parameters for the all data interval and VZA subset intervals. (Change Prob.: change probabilities; Conse.: number of consecutive anomaly observations.)

Parameters				**Accuracy Estimators**		
All data interval		**VZA subset intervals**				
Change Prob.	**Conse.**	**Change Prob.**	**Conse.**	**F1-score**	**Omission**	**Commission**
75.00%	14	75.00%	14	68.09%	31.16%	32.64%
75.00%	14	85.00%	14	68.18%	36.23%	26.75%
70.00%	16	80.00%	16	68.44%	36.23%	26.14%
70.00%	16	75.00%	14	68.58%	31.52%	31.32%
65.00%	16	85.00%	16	68.67%	34.78%	27.49%
70.00%	14	85.00%	14	68.73%	32.25%	30.26%
70.00%	16	85.00%	14	68.83%	35.87%	25.73%
70.00%	16	75.00%	16	69.00%	33.70%	28.08%
70.00%	16	85.00%	16	69.94%	36.59%	22.03%

4. Consistent dark pixel removal

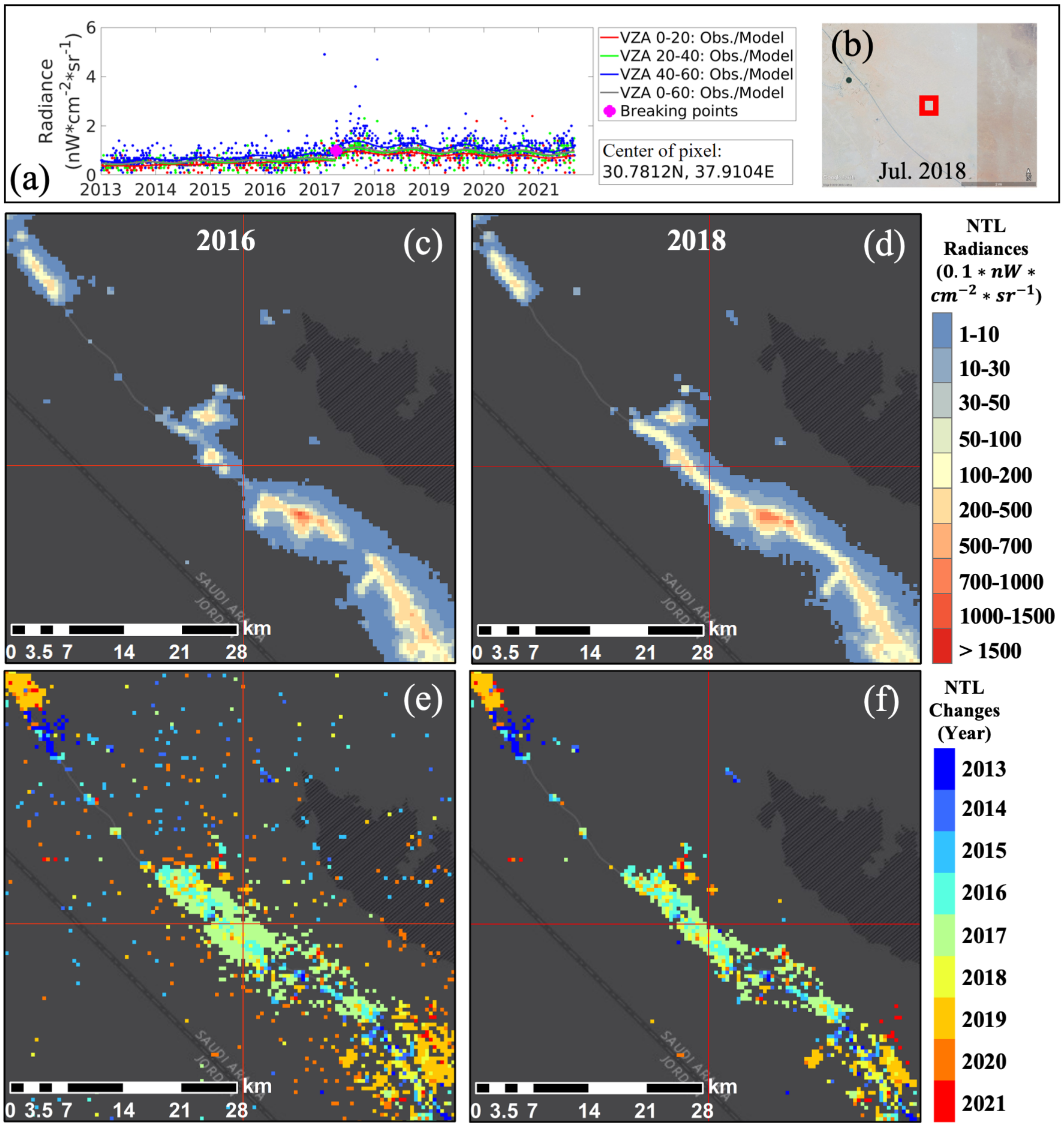

Fig. S3. Consistent dark pixel removal for a scattering light pixel. This pixel is located near a desert highway with improvements in electrification around 2017 in northwestern Saudi Arabia. (a) DNB time series at a dark barren pixel with a commission error before the consistent dark pixel removal was applied. The red, green, blue, and grey colors indicate the different VZA intervals, lines represent the estimated models, small dots are the DNB observations, and the large magenta dot is the detected change (red cross in Fig. S3e) that would be excluded by the dark pixel removal process (red cross in Fig. S3f). (b) The high-resolution Google Earth image in July 2018 for the selected pixel in Fig. S3a. The red rectangle represents the location and size of the selected pixel. (c) The Black Marble all angle snow-free annual composite NTL data (VNP46A4) around the selected pixel in 2016. (d) The black marble all angle snow-free annual composite NTL data (VNP46A4) around the selected pixel in 2018. (e) The accumulated annual NTL change maps before dark pixel removal. (f) The accumulated annual NTL change maps after dark pixel removal. The dark background in Fig. S3c-f is the Esri ArcMap Dark Gray Canvas base map.

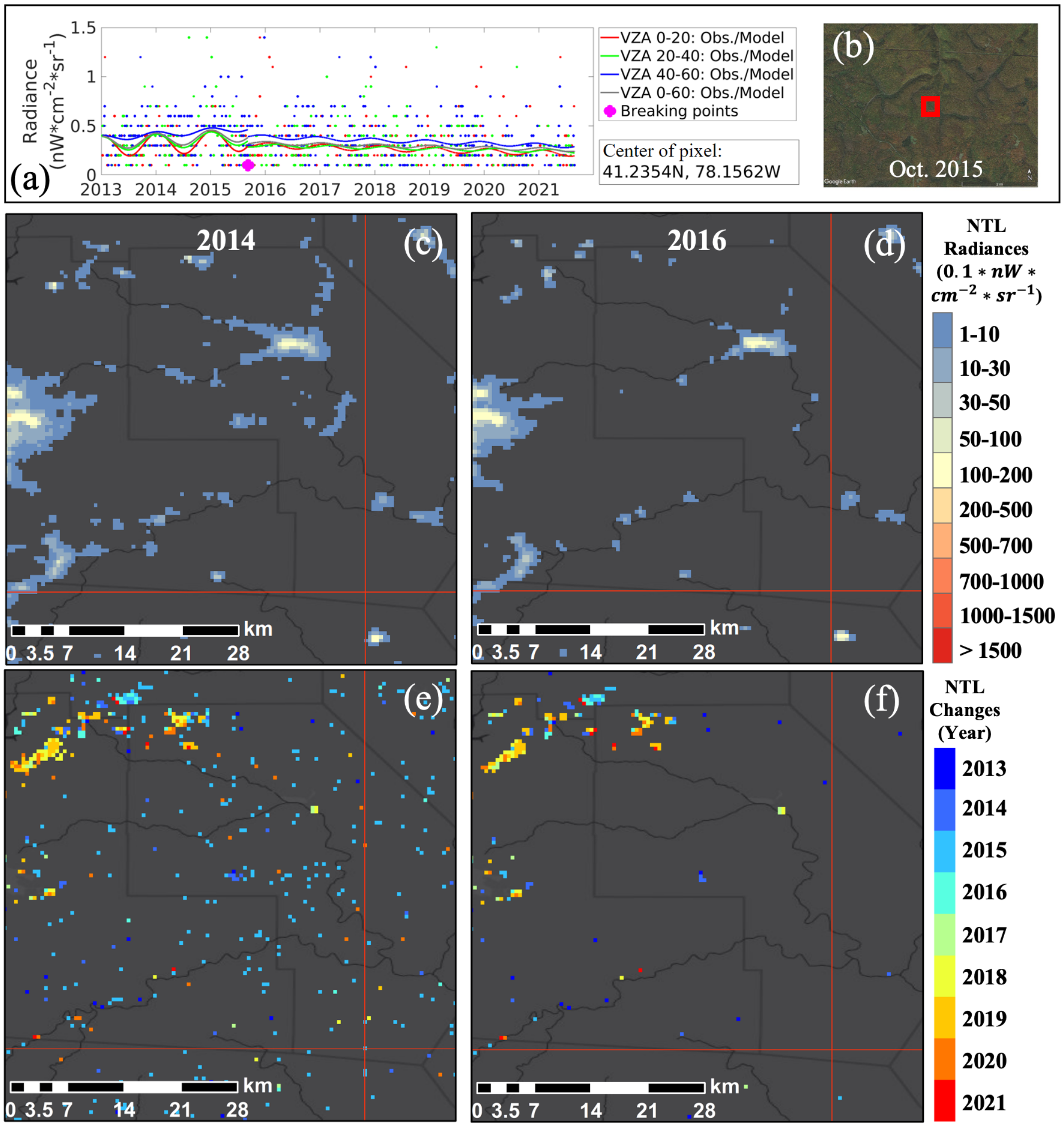

Fig. S4. Consistent dark pixel removal for a salt-and-pepper noise pixel. This pixel is in the vegetation areas of Mifflin, PA, US. (a) The DNB time series of a selected pixel with a commission error before the consistent dark pixel removal was applied. The red, green, blue, and grey colors indicate the different VZA intervals, lines represent the estimated models, small dots are the DNB observations, and the large magenta dot is the detected change (red cross in Fig. S4e) which would be excluded by the dark pixel removal (red cross in Fig. S4f). (b) The high-resolution Google Earth image in October 2015 for the selected barren pixel in Fig. S4a. The red rectangle represents the location and size of the selected pixel. (c) The black marble all angle snow-free annual composite NTL data (VNP46A4) around the selected pixel in 2014. (d) The Black Marble all angle snow-free annual composite NTL data (VNP46A4) around the selected pixel in 2016. (e) The accumulated annual NTL change maps before dark pixel removal. (f) The accumulated annual NTL change maps after dark pixel removal. The dark background in Fig. S4c-f is the Esri ArcMap Dark Gray Canvas base map.

5. Statistics of the validation samples

Table S2. Summary of 170 correctly detected and 2 missed NTL change validation samples based on their change type, land use/land cover, and change direction/magnitude. Note that only 164 validation samples were successfully interpreted to derive their change type and the corresponding land cover/use due to lack of high-resolution images for 8 of the validation samples. (mag.: magnitude; Omi.: omission error.)

ID	Human activities	Land use/land cover	Total (#)	Increase (#)	Average change mag. (nW*cm-2*sr-1)	Decrease (#)	Average change mag. (nW*cm-2*sr-1)	Omi. (#)
1	New construction	Residential	32	26	5.37	6	-8.65	0
		Non-residential	28	20	6.24	8	-2.31	0
2	Reconstruction	Residential	6	3	6.46	3	-1.99	0
		Non-residential	13	10	3.60	3	-0.52	2
3	Mining	Land cover change	6	3	1.25	3	-0.88	0
		No physical surface change	3	2	1.23	1	-8.74	0
4	Agriculture	Land cover change	7	6	0.96	1	-5.65	0
		No physical surface change	18	16	1.89	2	-2.22	0
5	Road	Land cover change	16	15	3.72	1	-1.63	0
		No physical surface change	2	2	1.21	0	Nan	0
6	Other	Residential	23	15	4.36	8	-3.49	0
		Non-residential	10	9	3.36	1	-16.90	0

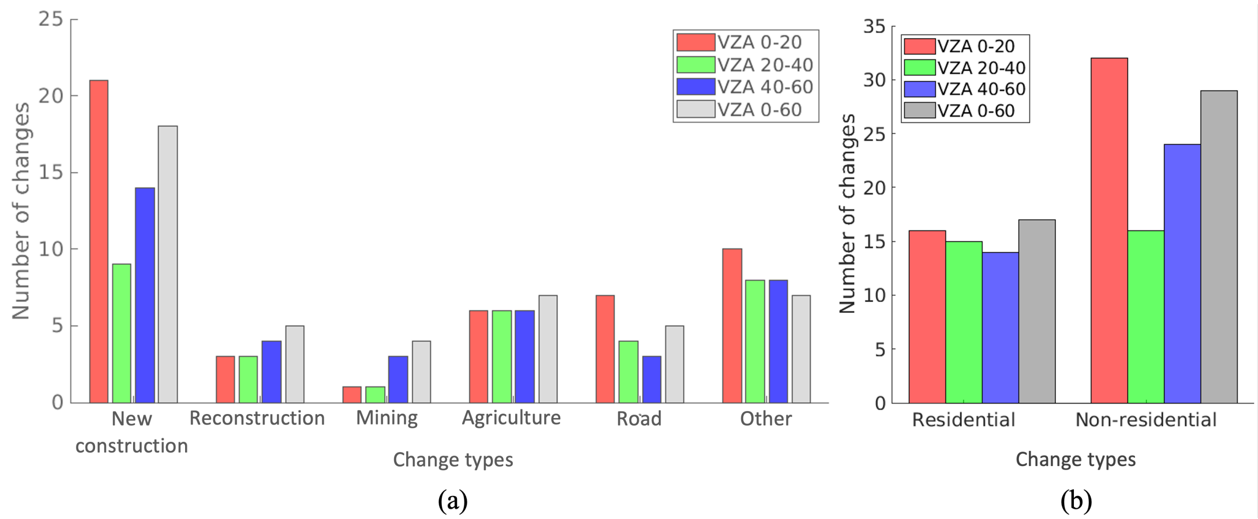

Fig. S5. Histograms of the correctly detected and successfully interpreted NTL change validation samples for different change types (a) and land cover/use (b) at different VZA intervals. The red, green, blue, and grey colors indicate the different VZA intervals that the changes were detected.